Supporting Information

Harnessing host–guest recognition and electron transfer in MXene–Fe_3O_4@Au–pillararene for enhanced 4-nitrophenol monitoring

Zhan Shu,[a,1] Tian Wang, [a,1] Jimei Chen,[a] Xinxin Zhang,[a] Xiting Zhu,[a] Jin Wang,[*a] Dongli Fan,[*a] Yang Wang,[a] Yong Yao,[a] and Mingshan Zhu,[*b]

[a]*School of Chemistry and Chemical Engineering, Nantong University, Nantong, 226019 (P. R. China) E-mail: wangjin107@ntu.edu.cn; fdlsky@ntu.edu.cn*

[b]*College of Environment and Climate, Jinan University, Guangzhou, 511443, China*

zhumingshan@jnu.edu.cn

1. Reagents and materials

Sodium dihydrogen phosphate dihydrate ($NaH_2PO_4.2H_2O$), ferric chloride ($FeCl_3$) and potassium ferricyanide ($K_3[Fe(CN)_6]$) were purchased from Shanghai Aladdin Biochemical Science and Technology Co. Sodium phosphate dibasic dodecahydrate ($Na_2HPO_4\cdot12H_2O$) was purchased from Guangdao Silong Chemical Co. Potassium ferricyanide ($K_4[Fe(CN)_6]$) were purchased from Shanghai McLean Biochemical Science and Technology Co. LiF and Ti_3AlC_2 were purchased from Nantong Feiyu Co., Ltd. Ultrapure water was used in all experiments.

2. Apparatus

High-Resolution Transmission Electron Microscope (HRTEM) and Transmission Electron Microscope (TEM) images were acquired via the TALOS (America). Scanning electron microscope (SEM) was scanned by Gemini SEM 3600 (Britain). UV-vis absorption spectra were measured using a Shimadzu UV-3600 spectrometer (Japan). X-ray photoelectron spectroscopy (XPS) was determined using the K-Alpha+(USA). Xray diffraction (XRD) was performed using a D8 advance X-ray diffractometer (Bruker AXS, Germany). The ultrasonic machine used in the experiment is PS-20A. All PEC experiments were conducted using the CHI660E electrochemical workstation (Shanghai Brilliance Instruments Co., Ltd.). The experiments were carried out using a conventional three-electrode system, with an RO232 saturated calomel electrode as the reference electrode, a 10 mm platinum mesh electrode as the counter electrode, and a 3 mm glassy carbon electrode as the working electrode.

3. Experimental section

3.1. Material preparation

3.1.1. Synthesis of Fe_3O_4 Microspheres:

$FeCl_3\cdot6H_2O$ (1.35 g, 5 mmol) was dissolved in ethylene glycol (40 mL) to form a clear solution. Subsequently, sodium acetate (NaAc, 3.6 g) and polyethylene glycol were added, and the mixture was vigorously stirred for 30 minutes. The solution was then transferred into a polytetrafluoroethylene (PTFE)-lined stainless-steel autoclave (50 mL capacity). The autoclave was heated to 200 °C and maintained at this temperature for 8-72 hours, followed by cooling to room temperature. The black product was washed several times with ethanol and dried at 60 °C for 6 hours.

3.1.2. Synthesis of Au NPs:

Briefly, 20 mL of 0.25 mM $HAuCl_4$ solution was placed in an ice-water bath. When the temperature reached approximately 0 °C, 0.60 mL of ice-cold 100 mM sodium borohydride ($NaBH_4$) solution was added dropwise. The mixture was stirred in the ice bath for 10 minutes, followed by additional stirring at room temperature for 3 hours to obtain gold nanoparticles (Au NPs). The Au NPs were stored at 4 °C.

3.1.3. Synthesis of multilayer $Ti_3C_2T_X$ MXene:

A mixture of 1.6 g LiF and 1 g Ti_3AlC_2 was placed in a polytetrafluoroethylene (PTFE) liner. The liner was then immersed in a constant-temperature water bath at 40 °C, followed by the addition of 20 mL of 9 M HCl for etching. After the reaction, the product was centrifuged (5000 rpm, 1 min) and washed until the supernatant reached pH=6. The resulting material was vacuum-dried at 70 °C to obtain multilayer MXene powder.

3.1.4. Synthesis of $CBpExP_6$

(1) Synthesis of compound A

1,4 - bis(2 - bromoethoxy)benzene (32.5 g) was weighed into a 500 mL round-bottom flask, followed by the addition of 150 mL of dichloromethane (DCM) to dissolve it. Then, $AlCl_3$ (2.6 g) was added to the flask. Subsequently, 4,4'-bis(chloromethyl)-1,1'-biphenyl (2.5 g) was weighed and dissolved in DCM in a beaker. The resulting solution was slowly added to the round-bottom flask via a constant-pressure dropping funnel over 1 hour. The reaction was allowed to proceed for an additional hour. After completion, the reaction mixture was quenched by pouring it into a 500 mL beaker containing a large amount of deionized water. The mixture was then transferred to a separatory funnel for phase separation. The organic phase was washed twice with water and twice with DCM. The resulting organic phase was dried over anhydrous sodium sulfate, filtered, and concentrated to obtain the crude product.

The crude product was purified by column chromatography using a mixture of petroleum ether/DCM (1:1) as the eluent, yielding 3 mg of a white solid (Compound A) with a yield of 36.5%.

^{1}H NMR (400 MHz, $CDCl_3$) δ (ppm): 7.48 (d, J = 8.1 Hz, 4H), 7.28 (d, J = 8.0 Hz, 4H), 6.79–6.75 (m, 4H), 4.22 (q, J = 6.2 Hz, 8H), 4.00 (s, 4H), 3.59 (td, J = 6.2, 3.6 Hz, 8H).

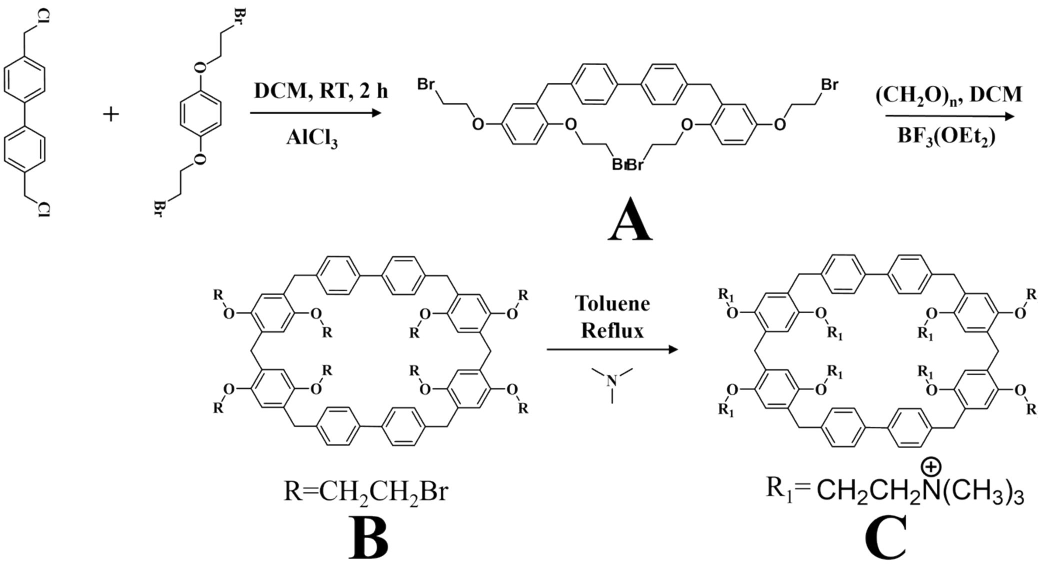

Fig. S1. Composite route of C.

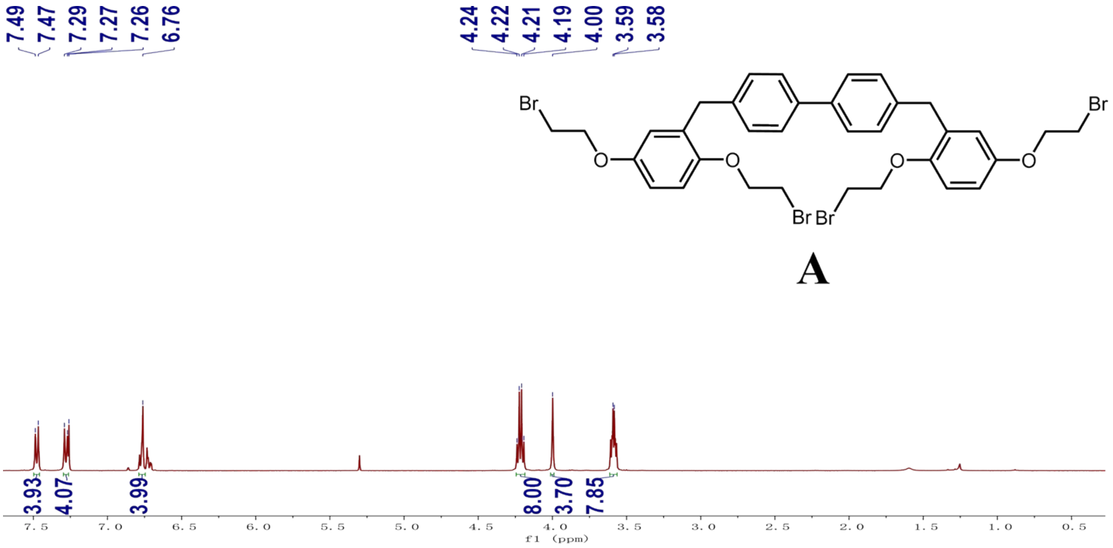

Fig. S2. ^{1}H NMR spectrum (400 MHz, $CDCl_3$, 293 K) of A.

(2) Synthesis of compound B

Compound A (1 g) was weighed into a 500 mL round-bottom flask and dissolved in 100 mL of dichloromethane (DCM). Paraformaldehyde (0.12 g) was then added to the flask, followed by the slow dropwise addition of boron trifluoride diethyl etherate

(2 mL). The reaction was monitored until the solution turned dark green, indicating completion. The reaction was quenched with saturated aqueous sodium bicarbonate, and the mixture was transferred to a separatory funnel for phase separation. The organic phase was washed three times with DCM and then dried over anhydrous sodium sulfate. After filtration and concentration, the crude product was obtained. Purification was carried out by column chromatography using a mixture of petroleum ether/DCM (1:1) as the eluent, yielding 350 mg of a white solid (Compound B) with a yield of 17.5%.

^{1}H NMR (400 MHz, $CDCl_3$) δ (ppm): 7.37 (d, J = 7.9 Hz, 8H), 7.21 (d, J = 8.0 Hz, 8H), 6.98 (s, 4H), 6.67 (s, 4H), 4.22 (dt, J = 22.1, 5.9 Hz, 16H), 3.95 (d, J = 4.7 Hz, 12H), 3.65 (t, J = 5.7 Hz, 8H), 3.51 (t, J = 6.2 Hz, 8H).

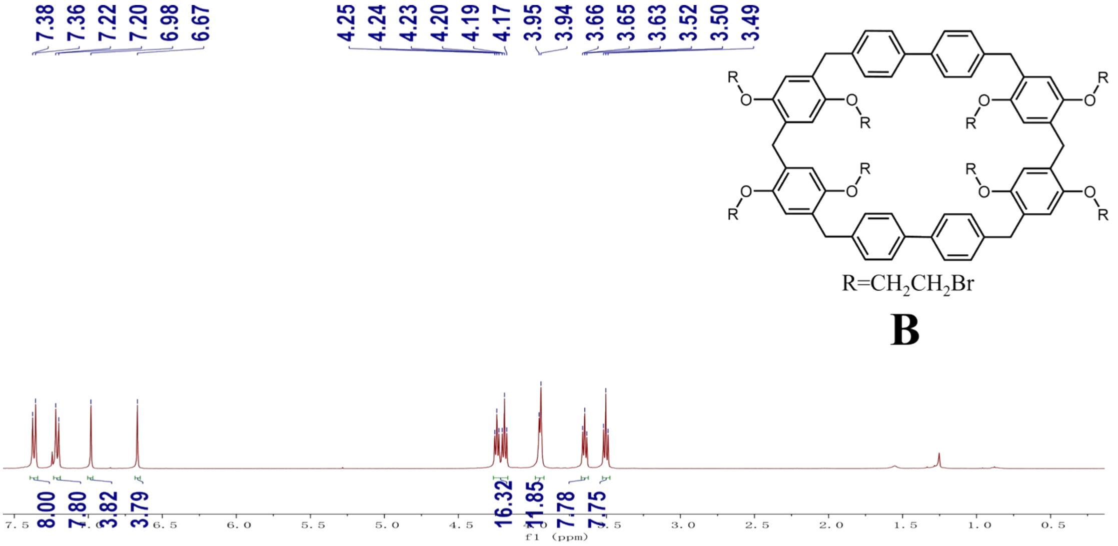

Fig. S3. ^{1}H NMR spectrum (400 MHz, $CDCl_3$, 293 K) of B.

(3) Synthesis of compound C

Compound B (500 mg) was weighed into a 250 mL round-bottom flask, followed by the addition of 60 mL of acetonitrile. Trimethylamine solution (2 mL) was then added, and the mixture was refluxed overnight. The reaction was considered complete when the initially milky-white solution turned colorless and transparent. The solution was then concentrated under reduced pressure. The resulting residue was dissolved in deionized water, and insoluble impurities were removed by filtration. The aqueous solution was subsequently concentrated to dryness, yielding 550 mg of a white solid product (Compound C) with a yield of 94%.

^{1}H NMR (400 MHz, D_2O) δ (ppm): 7.43 (d, J = 7.8 Hz, 8H), 7.18 (d, J = 7.8 Hz, 8H), 6.85 (s, 4H), 6.66 (s, 4H), 4.25 (d, J = 5.0 Hz, 8H), 4.18 (d, J = 5.9 Hz, 8H), 3.88 (d, J = 9.1 Hz, 12H), 3.52 (s, 16H), 2.93 (d, J = 14.4 Hz, 72H).

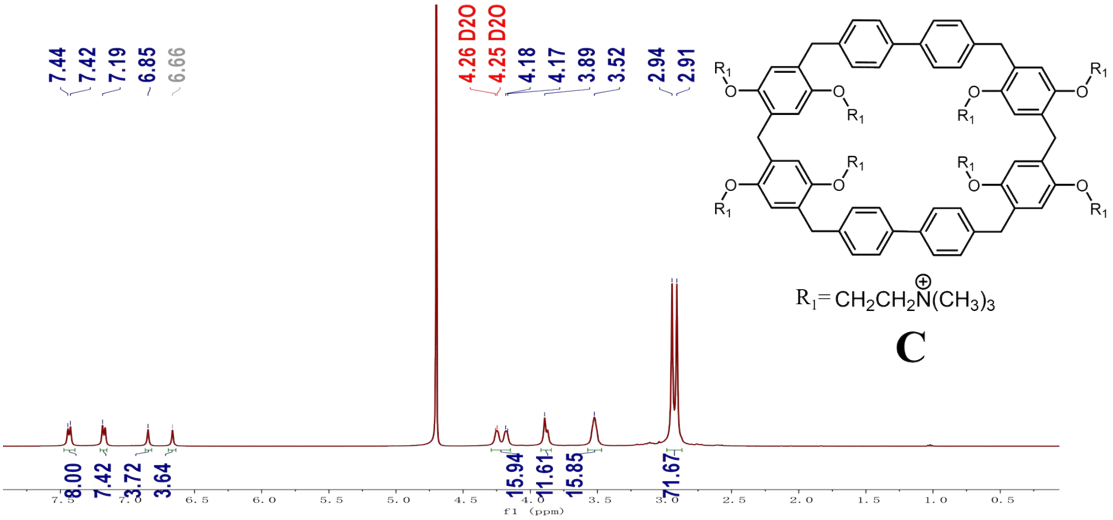

Fig. S4. ^{1}H NMR spectrum (400 MHz, D_2O, 293 K) of C.

3.2. Preparation of Fe_3O_4@Au@CBpExP$_6$/$Ti_3C_2T_X$ MXene composite material

5 mg of Fe_3O_4 nanoparticles were mixed with 2 mL of gold nanoparticles (Au NPs) solution. The mixture was subjected to magnetic sedimentation using an external magnet, allowing the Fe_3O_4@Au composite to settle at the bottom of the centrifuge tube. The supernatant was carefully removed, and the collected Fe_3O_4@Au nanoparticles were dried. The dried Fe_3O_4@Au nanoparticles were redispersed in 5 mL of deionized water. 5 mg of CBpExP6 was added to the suspension, where electrostatic adsorption facilitated the formation of Fe_3O_4@Au@CBpExP$_6$ composite nanoparticles. Finally, 10 mg of $Ti_3C_2T_X$ MXene was introduced into the Fe_3O_4@Au@CBpExP$_6$ dispersion, resulting in the formation of the Fe_3O_4@Au@CBpExP$_6$/$Ti_3C_2T_X$ MXene composite material.

3.3. The characterization of prepared materials

The chemical composition and bonding states of the Fe_3O_4@Au@CBpExP$_6$/Ti_3C_2TX MXene composite were investigated using X-ray photoelectron spectroscopy (XPS). Fig. S5A displays the high-resolution C 1s spectrum, which was deconvoluted into four distinct peaks at 288.68 eV (C=O), 286.23 eV (C–O), 284.78 eV (C–C), and 281.53 eV (C–Ti), confirming the presence of oxygen-containing functional groups and interfacial carbon-titanium bonding. In Fig. S5B, the N 1s spectrum exhibits two fitted peaks corresponding to N^+ (402.5 eV) and N–H (399.8 eV), providing strong evidence for the successful functionalization of $CBpExP_6$. The appearance of the N+ peak further indicates charge transfer interactions within the composite. The O 1s spectrum (Fig. S5C) reveals two major contributions at 532.03 eV (C=O) and 529.28 eV (C–O), consistent with the oxygenated carbon species observed in the C 1s spectrum. The Fe 2p spectrum (Fig. S5D) exhibits characteristic peaks for both Fe^{3+} (711.73 eV, $2p_{3/2}$; 723.93 eV, $2p_{1/2}$) and Fe^{2+} (714.08 eV, $2p_{3/2}$; 726.33 eV, $2p_{1/2}$), along with satellite features at 709.63 eV and 721.88 eV, confirming the mixed-valence state of iron in the Fe_3O_4 structure. Fig. S5E presents the Au 4f spectrum, where the spin-orbit doublet at 83.83 eV (Au $4f_{7/2}$) and 87.83 eV (Au $4f_{5/2}$) confirms the metallic Au (0) state, indicating the successful incorporation of gold nanoparticles. Finally, the Ti 2p spectrum (Fig. S5F) demonstrates multiple oxidation states, with peaks at 454.63 eV (Ti–C $2p_{3/2}$) and 463.38 eV (Ti–C $2p_{1/2}$) confirming the presence of Ti–C bonds in the MXene structure. Additional contributions at 455.93 eV (Ti^{2+} $2p_{3/2}$) and 460.88 eV (Ti^{2+} $2p_{1/2}$), along with a peak at 458.13 eV (Ti–O $2p_{3/2}$), suggest partial oxidation of the $Ti_3C_2T_X$ framework. The XPS survey spectrum (Fig. S6) further confirms the presence of all expected elements (Fe, Au, Ti, C, N, O), collectively validating the successful construction of the multicomponent nanocomposite.

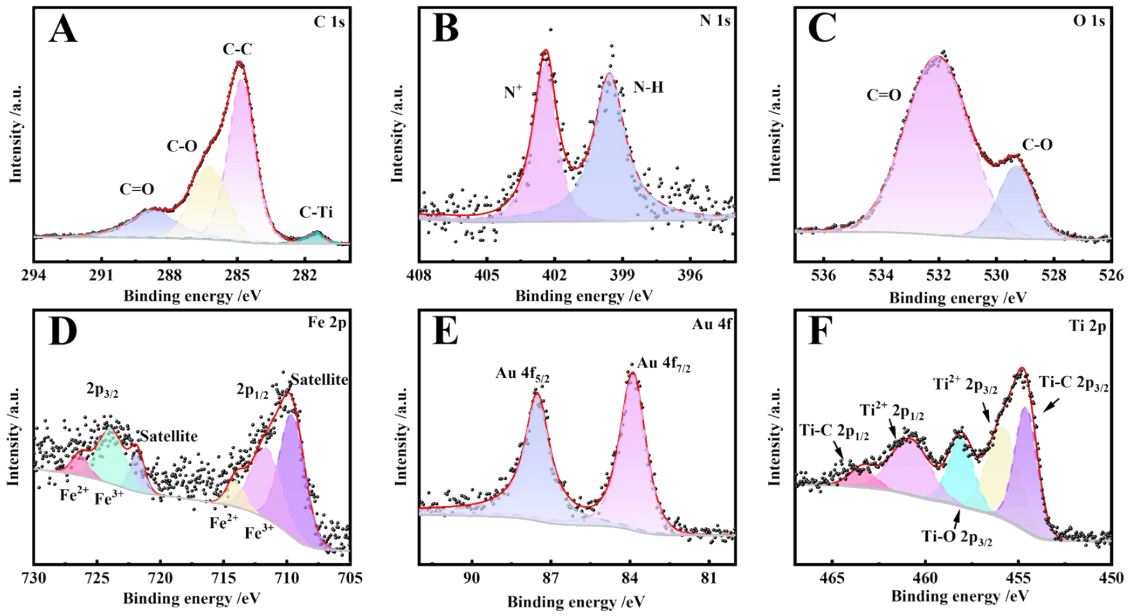

Fig. S5. XPS survey spectra of Fe_3O_4@Au@CBpExP$_6$/$Ti_3C_2T_X$ MXene (A) C 1s, (B) N 1s, (C) O 1s, (D) Fe 2p, (D) Au 4f, (D) Ti 2p.

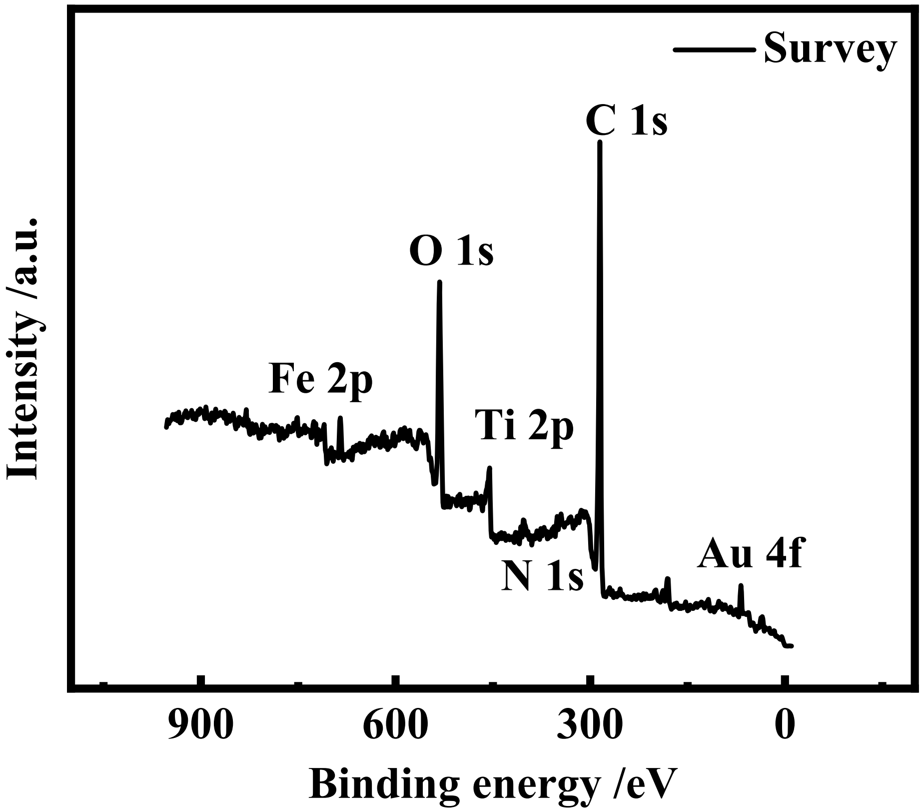

Fig. S6. Total XPS spectrum of Fe_3O_4@Au@CBpExP$_6$/$Ti_3C_2T_X$ MXene/GCE.

3.4. PEC measurement

The GCE on the suede surface was first polished with alumina polishing powder for 5 min, and then ultrasonic cleaned for 5 s in PS-20A ultrasonic cleaner with water and ethanol at a frequency of 40 kHz and 120 W respectively. To prepare the nanocomposite electrode, the composite material is dropped onto the treated GCE surface using a microsyringe and allowed to dry at 40 °C.

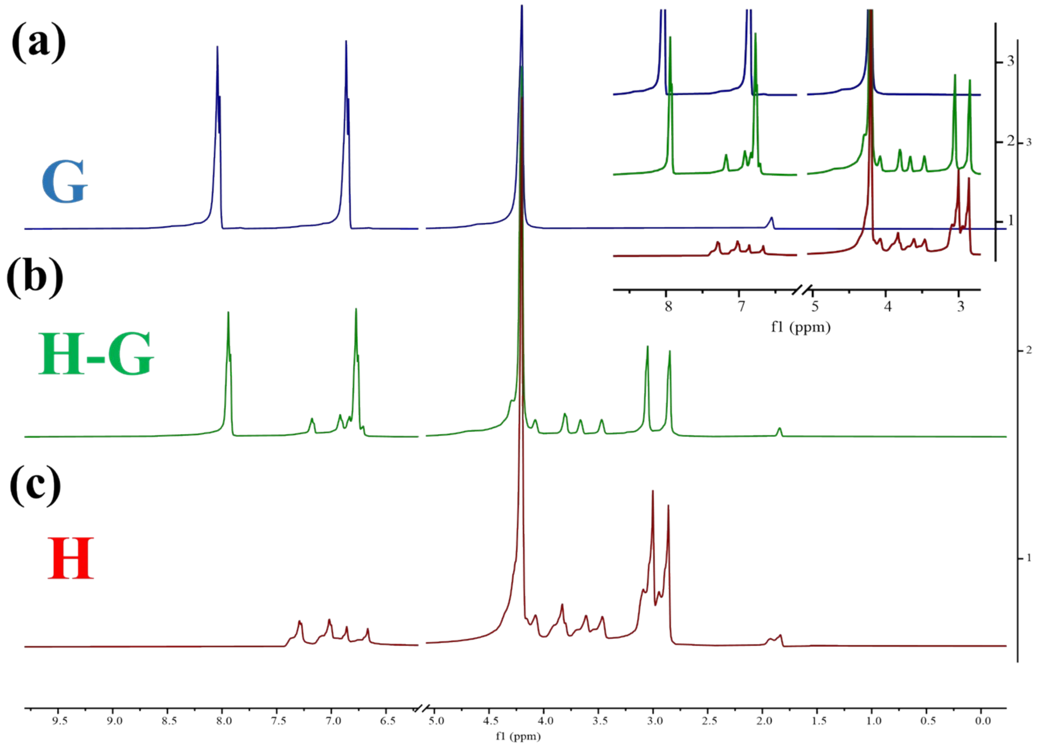

Fig. S7. ^{1}HNMR spectra (400 MHz, D_2O and C_2D_3N) of (a) G, (b) H-G, (c) H.

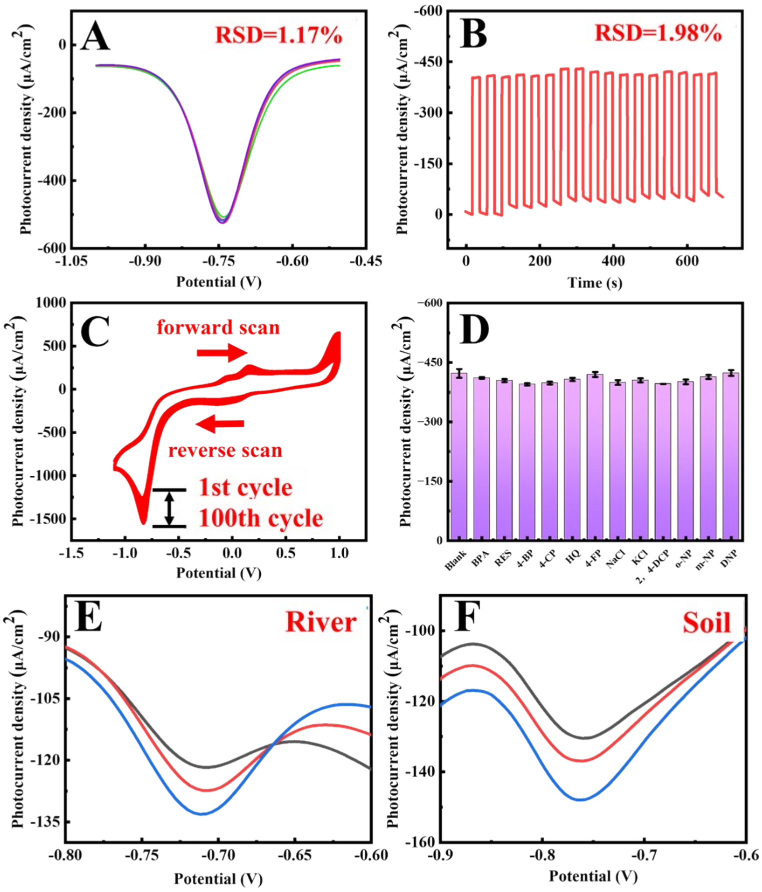

Fig. S8. (A) DPV responses of five identical electrodes in 0.5 mM 4-NP; (B) i-t response under intermittent illumination for 700 s; (C) CV curves from the 1st to 100th cycle in 0.5 mM 4-NP; (D) current response in the presence of 0.5 mM 4-NP with various interferents; (E–F) application of the sensor for 4-NP detection in river water (E), soil (F), and corresponding recovery results (n=3).

Table S1. Comparison of the present work with other reports for the detection of 4-NP.

Technique	Electrode	Linear range	Detection limit	Reference
Electrochemical method	BP/COF-NFs/GCE	0.1-200 µM	0.03 µM	[1]
Electrochemical method	CMS/GCE	2-1000 µM	0.2 µM	[2]
Electrochemical method	MoO_X/GCE	4-500 µM	0.0196 µM	[3]
Electrochemical method	（CeGdHfPrZr）O_2/GCE	5-100 µM	0.32 µM	[4]
Electrochemical method	CNF/CZO/ GCE	0.01-520 µM	0.2 µM	[5]
Photoelectrochemical method	Fe_3O_4@Au@CBpExP$_6$/$Ti_3C_2T_X$ MXene/GCE	1 nM-1.096 mM	0.33 nM	This work

Table S2. Application of the sensor for 4-NP detection in river water and soil.

Sample	add c(μM)	found c(μM) (n=3)	recovery(%)
Soil	30	28.22	94.07
	35	33.31	95.17
	40	42.22	105.55
River	20	21.13	105.65
	25	25.89	103.56
	30	30.42	101.4

References

1. H. Han, S. Zhang, S. Ding, D. Pan and N. Wang, *Sens. Actuators B Chem.*, 2025, **425**, 136998.
2. M. Yang, J. Feng, C. Li, Y. Wang and X. Zheng, *Microchem. J.*, 2025, **215**, 114407.
3. H.R. Li, H. Xu, Q.Y. Wang and S.-S. Li, *Talanta*, 2025, **285**, 127360.
4. M. Anandkumar, P. K. Kannan, R. S. Morozov, O. V. Zaitseva, S. Sudarsan and E. A.

Trofimov, *Ceram. Int.*, 2025, **51**, 2770-2778.

5. K. Mariappan, S. Sakthinathan, S.M. Chen and T.W. Chiu, *Colloids Surf. A*, 2024, **685**, 133147.